Heme Oxygenase-1 Induction Remodels Adipose Tissue and Improves Insulin Sensitivity in Obesity-Induced Diabetic Rats

Angelique Nicolai, Ming Li, Dong Hyun Kim, Stephen J. Peterson, Luca Vanella, Vincenzo Positano, Amalia Gastaldelli, Rita Rezzani, Luigi F. Rodella, George Drummond, Claudia Kusmic, Antonio L'Abbate, Attallah Kappas and Nader G. Abraham

Hypertension 2009;53;508-515; originally published online Jan 26, 2009;
DOI: 10.1161/HYPERTENSIONAHA.108.124701
Hypertension is published by the American Heart Association. 7272 Greenville Avenue, Dallas, TX 72514
 Print ISSN: 0194-911X. Online ISSN: 1524-4563

Heme Oxygenase-1 Induction Remodels Adipose Tissue and Improves Insulin Sensitivity in Obesity-Induced Diabetic Rats

Angelique Nicolai, Ming Li, Dong Hyun Kim, Stephen J. Peterson, Luca Vanella, Vincenzo Positano, Amalia Gastaldelli, Rita Rezzani, Luigi F. Rodella, George Drummond, Claudia Kusmic, Antonio L'Abbate, Attallah Kappas, Nader G. Abraham

Abstract—Obesity-associated inflammation causes insulin resistance. Obese adipose tissue displays hypertrophied adipocytes and increased expression of the cannabinoid-1 receptor. Cobalt protoporphyrin (CoPP) increases heme oxygenase-1 (HO-1) activity, increasing adiponectin and reducing inflammatory cytokines. We hypothesize that CoPP administration to Zucker diabetic fat (ZDF) rats would improve insulin sensitivity and remodel adipose tissue. Twelve-week-old Zucker lean and ZDF rats were divided into 4 groups: Zucker lean, Zucker lean–CoPP, ZDF, and ZDF–CoPP. Control groups received vehicle and treatment groups received CoPP (2 mg/kg body weight) once weekly for 6 weeks. Serum insulin levels and glucose response to insulin injection were measured. At 18 weeks of age, rats were euthanized, and aorta, kidney, and subcutaneous and visceral adipose tissues were harvested. HO-1 expression was measured by Western blot analysis and HO-1 activity by serum carbon monoxide content. Adipocyte size and cannabinoid-1 expression were measured. Adipose tissue volumes were determined using MRI. CoPP significantly increased HO-1 activity, phosphorylated AKT and phosphorylated AMP kinase, and serum adiponectin in ZDF rats. HO-1 induction improved hyperinsulinemia and insulin sensitivity in ZDF rats. Subcutaneous and visceral adipose tissue volumes were significantly decreased in ZDF rats. Adipocyte size and cannabinoid-1 expression were both significantly reduced in ZDF–CoPP rats in subcutaneous and visceral adipose tissues. This study demonstrates that HO-1 induction improves insulin sensitivity, downregulates the peripheral endocannabinoid system, reduces adipose tissue volume, and causes adipose tissue remodeling in a model of obesity-induced insulin resistance. These findings suggest HO-1 as a potential therapeutic target for obesity and its associated health risks. **(*Hypertension*. 2009;53:508-515.)**

Key Words: insulin resistance ■ heme oxygenase-1 ■ adiponectin ■ adiposity ■ endocannabinoid ■ pAMPK

Obesity is increasingly recognized as a chronic inflammatory condition[1] in which the detrimental effects on metabolic function are mediated, at least in part, by an upregulation of inflammatory molecules. Adipose tissue production and secretion of inflammatory proteins such as tumor necrosis factor-α and interleukin-6, as well as the generation of reactive oxygen species, have been linked to increased insulin resistance.[2,3] Visceral adipose tissue (VAT), the cause of central obesity and one of the features of the metabolic syndrome, plays a more dominant role in obesity-induced, inflammation-mediated insulin resistance compared with subcutaneous adipose tissue (SAT).[1] Indeed, Kim et al showed significant improvement in multiple parameters associated with the metabolic syndrome, including insulin resistance, despite an almost unlimited expansion of SAT and in the absence of a concomitant increase in VAT.[4] In VAT, increased cannibinoid-1 (CB-1) receptor activity leads to a decrease in adiponectin and an increase in lipogenesis, both of which contribute to insulin resistance. The CB-1 receptor is a regulatory protein linked to abnormal glucose levels and obesity that has shown to increase hepatic lipogenic transcription factor and fatty acid synthesis.[5] Consequently, CB-1 levels could be an indicator of the adiposity state.

The heme oxygenase (HO) system exerts antioxidant and antiapoptotic effects via its end-products bilirubin/biliverdin and carbon monoxide (CO).[6,7] Whereas HO-2 is expressed constitutively, HO-1 is an inducible molecule, produced in response to oxidative stress, which has been shown to slow weight gain, decrease levels of tumor necrosis factor-α and

Received October 7, 2008; first decision October 22, 2008; revision accepted December 6, 2008.

From the Departments of Pharmacology (A.N., M.L., D.H.K., S.J.P., L.V., G.D., N.G.A.) and Medicine (S.J.P., N.G.A.), New York Medical College, Valhalla; Scuola Superiore Sant'Anna and Consiglio Nazionale delle Ricerche Institute of Clinical Physiology (V.P., A.G., C.K., A.L.), Pisa, Italy; University of Brescia (R.R., L.F.R.), Italy; and Rockefeller University (A.K.), New York.

The first 2 authors contributed equally to this work.

This work was presented in part to the American Heart Association 62nd High Blood Pressure Research Council, September 17–20, 2008.

Correspondence to Dr Nader G. Abraham, Professor of Pharmacology and Medicine, Department of Pharmacology, New York Medical College, Valhalla, NY 10595 or Dr Attallah Kappas, Rockefeller University, New York, NY 10021. E-mail nader_abraham@nymc.edu

Hypertension **is available at http://hyper.ahajournals.org** **DOI: 10.1161/HYPERTENSIONAHA.108.124701**

interleukin-6, and increase serum levels of adiponectin in obese rats and obese diabetic mice.[6,8] The association observed between HO-1 and adiponectin has led to the proposal of an HO-1–adiponectin axis.[8]

The Zucker diabetic fat (ZDF) rat is a model of insulin resistance characterized by hyperinsulinemia, hyperglycemia, hyperlipidemia, moderate hypertension, and obesity.[9] In the present study, we hypothesize that upregulation of the HO system with the HO-1 inducer cobalt protoporphyrin (CoPP) would increase adiponectin levels, improve insulin sensitivity via increased AMP kinase (AMPK) phosphorylation, decrease adipose tissue volumes, and cause adipose tissue redistribution and remodeling in the ZDF model of obesity-induced insulin resistance.

Methods

Animal Protocols

Male ZDF and lean rats (Charles River Laboratory; Wilmington, Mass) were maintained on a standard rat diet and given tap water ad libitum. Rats were divided into 4 groups: lean, lean-CoPP, ZDF, ZDF–CoPP (n=5 in each group). ZDF and age-matched lean rats were treated with CoPP (2 mg/kg body weight, once weekly), administered via intraperitoneal injection from the onset of diabetes (age 12 weeks) for 6 weeks. Animals were euthanized at 18 weeks of age, 2 days after the final injection. At euthanization, SAT and VAT in the abdomen (the visible mesenteric fat, fat around the liver, kidney, and spleen) were dissected free, pooled for each rat, and weighed.

Glucose monitoring was performed using an automated analyzer (Lifescan Inc). Food intake did not change in the treatment groups. The animal care and use committee of New York Medical College approved all experiments.

Magnetic Resonance Imaging

SAT and VAT were determined by MRI, whereas hepatic fat was determined by magnetic resonance spectroscopy. Rats were imaged in a General Electric excite 1.5T scanner using a knee coil with a T1-weighted spin-echo pulse sequence (TEC, 9.0 ms; repetition time, 540 ms; number of excitations, 4; field of view, 8×8 cm; image size, 224×192 pixels). The whole chest and abdomen of each rat were covered with axial slices (3-mm thick, no spacing). Acquired images underwent semiautomatic segmentation of SAT and VAT using the previously validated HIPPO FAT tool.[10–12]

The software computed 3 masks (background, fat, and nonfat tissues) using a fuzzy clustering segmentation. After this step, external and internal SAT boundaries were defined by an active contour algorithm that exploited the previously computed masks as external force maps. A third contour was computed surrounding the area where VAT was present together with other tissues. VAT itself was assessed by the automated analysis of the signal histogram in the visceral region defined previously by identifying the second peak of the signal histogram. This provided whole body volume (including the skeletal and soft tissues), total fat, SAT, and VAT volumes, VAT/SAT ratio, and fat/body volume ratio.[10–12]

Tissue Preparation for Western Blot in Kidneys and Aorta

At the time of euthanization, aorta and kidney tissues were harvested, drained of blood, and flash-frozen in liquid nitrogen. Specimens were maintained at −80°C until needed. Frozen aorta and kidney segments were pulverized and placed in a homogenization buffer (10 mmol/L phosphate buffer, 250 mmol/L sucrose, 1 mmol/L EDTA, 0.1 mmol/L PMSF, and 0.1% tergitol, pH 7.5). Homogenates were centrifuged at 27 000*g* for 10 minutes at 4°C, supernatant was isolated, and protein levels were visualized by immunoblotting with antibodies. Antibodies against phosphorylated AMPK (pAMPK) were obtained from Cell Signaling Technology. Antibodies were prepared by dilution of HO-1, HO-2, and pAMPK as we described previously.[6,8,13]

Assessment of CO Formation

CO formation will be measured in vascular tissues. Arterial specimens will be cut into 2-mm segments and transferred into amber glass vials (2 mL) containing 1.0 mL of Krebs' buffer saturated with 95% O_2 and 5% CO_2 with and without heme or HO inhibitors (chromium mesoporphyrin [CrMP]). The vials will be capped tightly with rubberized Teflon liners, and the samples will be incubated at 37°C for 1 hour. Subsequently, the vials will be placed on ice, and the internal standard will be added. CO content in the headspace will be determined as described above. CO-generating activity will be expressed as pmol/mg protein per hour. Values obtained in the absence of NADPH (NADPH-independent CO generation) will be subtracted from values in the presence of NADPH (total CO generation); the resulting values represent the NADPH-dependent generation of CO, which is an index of HO activity, as we described previously.[14,15]

Cytokine Measurements

Serum adiponectin (high molecular weight) was determined in rat plasma using an ELISA assay (Pierce Biotechnology, Inc).

Insulin Tolerance Test

After a 6-hour fast, rats were injected intraperitoneally with insulin (2.0 U/kg). Blood samples were taken at various time points (0 to 90 minutes), and blood glucose levels were measured.

Tissue Preparation for Fat Determination and Histological Analysis

At the time of euthanization, SAT and VAT in the abdomen (the visible mesenteric fat, fat around the liver, fat around the kidney, and fat around the spleen) were dissected free, pooled for each rat, and weighed. Subcutaneous and visceral aortic adipose tissues collected from ZDF control and ZDF–CoPP rats (4 animals per group) were prepared for morphological analysis. Samples were fixed in 4% paraformaldehyde for 24 hours, cut into small pieces, and embedded in paraffin for histological analysis. The samples were cut by microtome (5-μm thick), mounted on D-polylisinated glass slides, deparaffinized in xylene, and stained with hematoxylin and eosin for the evaluation of adipocyte size or processed for CB-1 or HO-1 immunohistochemistry.

Evaluation of Adipocyte Size

Digital images of adipose tissue sections were captured using a light microscope (Olympus) at ×20 magnification. For each group, 3 fields from each of 5 different hematoxylin-eosin–stained sections per animal were analyzed. Individual adipocyte areas (μm^2) within each field were determined using image analysis software (Image Pro Plus; Immagini e Computer). For the quantitative analysis, adipocyte areas were calculated in arbitrary fields, measuring 50 adipocytes for each section.

Immunohistochemistry

Immunostaining of adipose tissue for CB-1 or HO-1 was performed using a goat polyclonal anti–CB-1 primary antibody[16] (Santa Cruz Biotechnology) or a rabbit polyclonal anti–HO-1 primary antibody (StressGen Biotechnologies). For each experimental group, 5 sections per animal were stained. Sections were immersed in 3% hydrogen peroxide and diluted in methanol for 30 minutes to quench endogenous peroxidase activity. Sections were preincubated with 3% horse (for CB-1) or goat (for HO-1) serum for 60 minutes, followed by primary antibody anti–CB-1 diluted 1:125 or primary antibody anti–HO-1 diluted 1:500 for 2 hours at 37°C. The sections were then washed in Tris-buffered saline (0.1 mol/L), incubated for 30 minutes at room temperature with biotinilated horse anti-goat immunoglobulin (for CB-1; Vector Laboratories; Burlingame, Calif) or goat

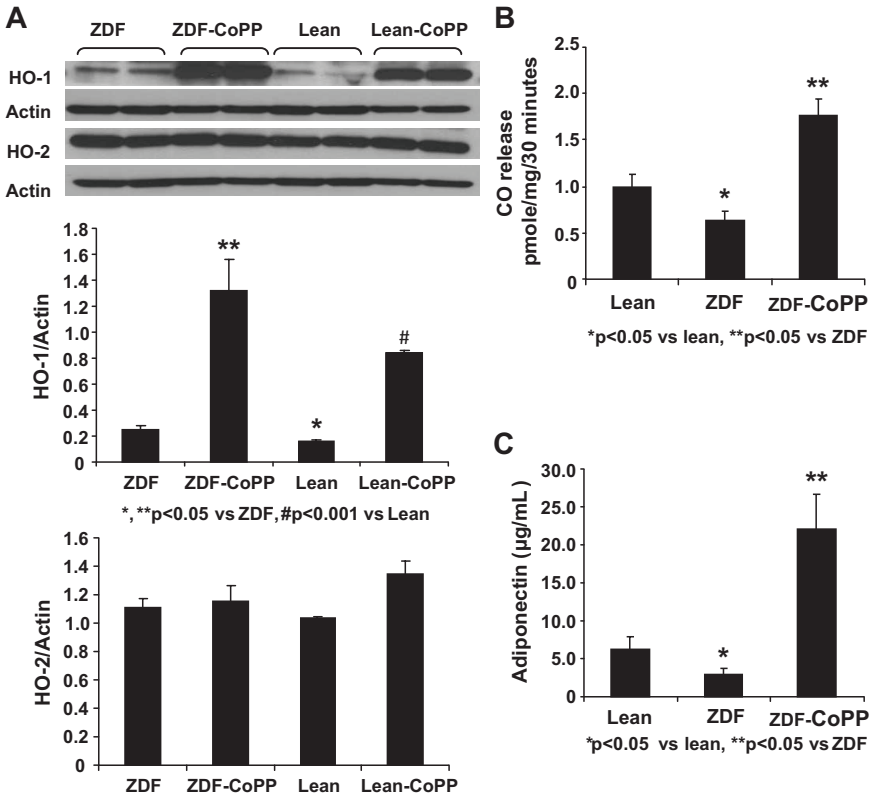

Figure 1. A, Aortic tissue homogenates were subjected to Western blotting for HO-1 and HO-2 protein determination and densitometry analyses of HO-1 and HO-2/actin ratio. *$P<0.05$; **$P<0.05$ vs ZDF rats; #$P<0.001$. CoPP was administered once per week for 6 weeks. B, CO levels were lower in ZDF control rats. Results are mean±SE; n=4. CO release was determined as in Methods and expressed as pmol/mg per 30 minutes. Significance levels were *$P<0.05$ lean vs ZDF rats and **$P<0.05$ vs ZDF rats. C, Effect of CoPP on serum adiponectin levels in lean, ZDF, and ZDF–CoPP rats. CoPP was administered weekly for 6 weeks, and serum samples were obtained immediately before euthanization. Results are expressed as μg/mL serum; mean±SE; n=8 to 12. Significance levels were *$P<0.05$ lean vs ZDF rats and **$P<0.005$ ZDF vs ZDF–CoPP rats.

anti-rabbit immunoglobulin (for HO-1; Vector Laboratories), and then for 30 minutes at room temperature with avidin-biotin–horseradish peroxidase complex (Vector Laboratories). The reaction product was visualized using hydrogen peroxide and diaminobenzidine (Sigma) as a chromogen. All slides were dehydrated and mounted in DPX (Sigma). Negative controls performed substituting primary antibody with nonimmune serum revealed no signal.

Evaluation of CB-1 and HO-1 Immunostaining and Statistical Analysis

CB-1 and HO-1 staining intensity was computed as integrated optical density (IOD). Digitally fixed images of the slices (n=5 per animal) at ×20 magnification were analyzed using an optical microscope (Olympus) equipped with an image analyzer (Image Pro Plus; Immagini e Computer). For quantitative analysis, IOD was calculated for arbitrary areas, measuring 3 fields with the same area for each section.

Statistical Analyses

Statistical significance between experimental groups was determined by the Fisher method of analysis of multiple comparisons, with $P<0.05$ considered significant. For comparison between treatment groups, the null hypothesis was tested by a single-factor ANOVA for multiple groups or unpaired *t* test for 2 groups, and data are presented as mean±SE.

Results

Effect of CoPP on HO-1 and Adiponectin Expression

As seen in Figure 1A, the HO-1/actin ratio in aorta lean controls (0.150±0.010) was significantly less than in ZDF controls (0.255±0.023; $P<0.05$). Treatment with CoPP significantly increased aorta HO-1 levels in both ZDF and lean rats. The HO-1/actin ratio in lean rats treated with CoPP (0.838±0.023) was significantly higher than in lean controls ($P<0.001$). The ratio was also elevated in ZDF rats treated with CoPP (1.322±0.237) compared with ZDF controls ($P<0.05$). At the same time, CO levels, an indicator of total HO activity, were decreased in ZDF rats compared with lean controls, suggesting that HO-1 is inactivated by obese/hyperglycemic conditions. CoPP administration increased CO in ZDF rats to levels greater than those in lean controls, indicating an increase in HO-1 activity (Figure 1B).

Similarly, plasma levels of adiponectin were significantly lower in ZDF control rats (2.9±0.74 μg/mL) compared with lean controls (6.2±1.84 μg/mL; $P<0.05$). HO-1 induction with CoPP markedly increased adiponectin levels in ZDF rats (22.1±4.5 μg/mL) compared with untreated ZDF animals ($P<0.05$; Figure 1C). However, HO-1 induction did not significantly change adiponectin levels in lean rats (data not shown).

Effect of CoPP on Insulin Sensitivity

ZDF control rats demonstrated marked hyperinsulinemia compared with lean controls, with serum insulin concentrations of 475.3±188.6 pM and 221.1±36.2 pM, respectively ($P<0.05$). HO-1 induction corrected this difference, reducing insulin levels to 224.5±25.5 pM in ZDF–CoPP rats ($P<0.05$). Similarly, CoPP improved insulin sensitivity as demonstrated by the striking response in glucose levels of ZDF–CoPP rats to insulin administration compared with ZDF controls (Figure 2).

Effect of HO-1 Induction on Weight Gain and Adipose Tissue Volumes

HO-1 and adiponectin induction significantly reduced weight gain in ZDF rats treated with CoPP compared with ZDF

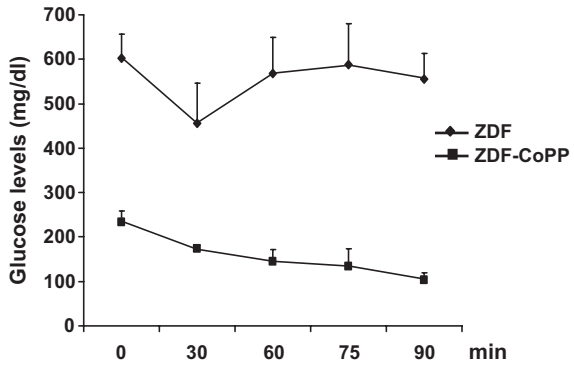

Figure 2. Effect of HO-1 expression on insulin sensitivity. Intraperitoneal insulin sensitivity tests were performed on ZDF controls and ZDF–CoPP rats as described in Methods. Results are expressed as mean±SEM; n=3. *$P<0.05$; **$P<0.01$ ZDF vs ZDF–CoPP rats.

controls. Figure 3 depicts representative samples of each of the 4 treatment groups, with the VAT dissected from each at the time of euthanization. Body weight and SAT and VAT weights were reduced significantly in the ZDF–CoPP rats compared with ZDF controls. At 12 weeks of age, the ZDF control group had an average total body weight of 470±4 g, which had increased to 607±17 g by 18 weeks of age. The ZDF–CoPP group had an average body weight of 457±10 g at 12 weeks of age and remained relatively stable at 424±31 g at 18 weeks of age.

The SATs and VATs dissected at euthanization were pooled and weighed for each rat. SAT weight in ZDF controls

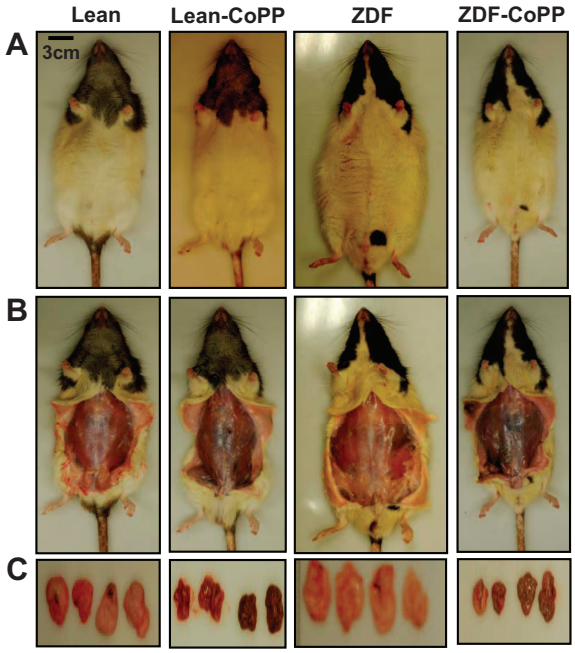

Figure 3. Effect of CoPP on body weight appearance and visceral fat content in lean, lean–CoPP, ZDF, and ZDF–CoPP rats. A, Effect of CoPP administration on body appearance. B, Examination of SAT and examples of SAT and VAT. C, Dissected fat from lean and ZDF rats. Representative photographs show 1 rat from each group after 6 weeks of treatment (n=8) and untreated ZDF, ZDF–CoPP, and obese–CoPP rats after 6 weeks of treatment.

(8.9±0.7 g) was decreased to 5.6±1.9 g in ZDF–CoPP rats ($P<0.05$). Most significantly, VAT weight in ZDF controls was 17.73±1.35 g and decreased ≈63% to 6.61±1.59 g in ZDF–CoPP rats ($P<0.05$).

Effect of CoPP on Fat Content Determined by MRI

Visual inspection and dissection of visceral fat around various organs and dissection of SAT provide semiquantitative estimates of fat content. MRI was used to quantify SAT and VAT.

Figure 4 depicts a sagital MRI of a ZDF control rat and representative axial cross-sections from a ZDF control and ZDF–CoPP rat, with VAT highlighted in red (top). MRI and HIPPO FAT analysis demonstrated a significant reduction in SAT. As seen in Figure 4, global SAT and VAT were significantly decreased in ZDF–CoPP rats compared with ZDF untreated rats ($P<0.04$ and $P<0.02$, respectively).

Effect of HO-1 Induction on Adipocyte Histology

To confirm the effects of CoPP on HO-1 expression in adipose tissue, adipocytes from ZDF control and ZDF–CoPP animals were stained for HO-1 expression. HO-1 staining optical density was increased in both SAT and VAT in ZDF rats treated with CoPP compared with ZDF controls ($P<0.05$; Figure 5A and 5B).

As shown in Figure 5C, the average cross-sectional area of subcutaneous adipocytes from ZDF control rats was 5221.871±1367.878 μm^2. This area was significantly reduced ($P<0.05$) in the subcutaneous adipocytes obtained from ZDF–CoPP rats (3553.136±1036.699 μm^2). Although the average adipocyte size in VAT (3744.738±971.195 μm^2) was smaller than in SAT in ZDF controls, HO-1–adiponectin induction still significantly reduced visceral adipocyte size (2626.998±765.105 μm^2; $P<0.05$).

Immunostaining for the CB-1 receptor was performed on SAT and VAT in ZDF control and ZDF–CoPP rats. As shown in Figure 5D, compared with ZDF controls, HO-1–adiponectin induction significantly reduced ($P<0.05$) CB-1 expression in SATs (IOD, 595.45±119.04 versus 520.25±105.4, respectively) and VATs (IOD, 788.77±124.44 versus 589.45±153.82, respectively), with a more pronounced decrease in CB-1 expression in VAT. These changes in CB-1 expression were not accompanied by a significant change in food intake between control and CoPP groups (data not shown).

Effect of HO-1 Induction on pAMPK Levels

Figure 6 represents Western blot analysis of the levels of pAMPK and phosphorylated AKT (pAKT) in aorta and kidney tissues from lean control, lean–CoPP, ZDF control, and ZDF–CoPP animals. pAKT and AMPK phosphorylation was reduced in ZDF controls compared with lean animals. Although HO-1 induction increased both pAKT and pAMPK levels in ZDF rats ($P<0.05$), there was not a significant difference in AMPK phosphorylation and pAKT between lean control rats and lean rats treated with CoPP.

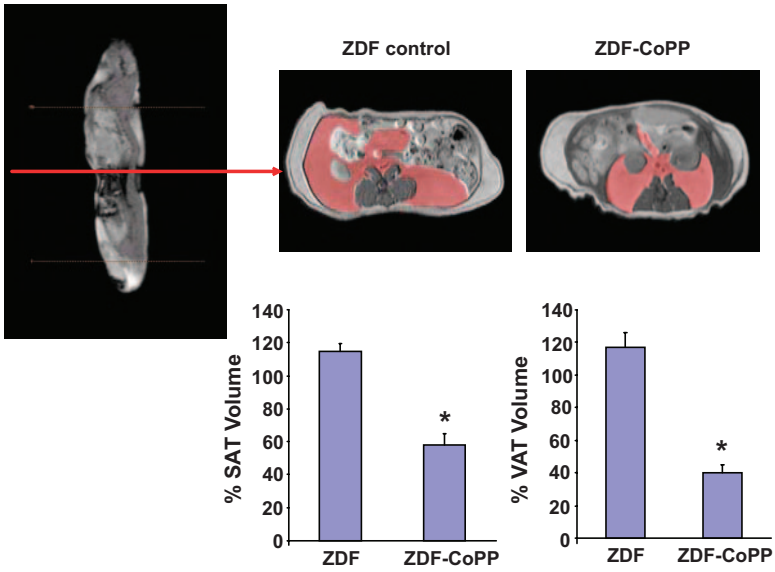

Figure 4. MRI sagital image with representative axial cross sections of a ZDF control and ZDF–CoPP rat. VAT is highlighted in red (top). Percent decrease in adipose tissue volumes is represented graphically. HO-1 induction significantly reduced SAT and VAT volumes. *$P<0.05$; n=4.

Discussion

In the present report, we demonstrate that HO-1 induction improved insulin sensitivity and decreased adiposity, resulting in a decrease in both SAT and VAT volumes, with increased numbers of adipocytes that were significantly smaller in size. Both improved insulin sensitivity and adipose tissue remodeling were accomplished by HO-1 induction via a mechanism that involves increased levels of adiponectin and pAMPK. We have shown previously that an increase in cardiac HO-1 proteins levels increases serum adiponectin and enhances pAKT.[17] A large body of evidence has shown that activated AMPK and phosphatidylinositol 3-kinase/AKT signaling participates in regulation of cell survival and protects against oxidative stress.[18–21] Activation of AMPK and pAKT increases phosphorylation of several target molecules that results in increased glucose transport, fatty acid oxidation,[22,23] and phosphorylated endothelial nitric oxide synthase (eNOS).[24] Thus, HO-1 induction appears capable of reprogramming adipocytes in a manner that results in the expression of a new phenotype that is better able to respond to insulin and restore insulin sensitivity. This phenomenon is similar to the response of vascular tissue to HO-1 induction that has already been observed.[8,16,25,26] We reported previously the effects of HO-1 induction on adiponectin levels, inflammatory cytokine levels, and weight gain in the ZDF model.[6] The new results reported here extend the purview of our previous findings, indicating that upregulation of the HO-1/adiponectin system exerts beneficial effects on obesity-induced insulin resistance.

Western blot analysis and CO assays of aorta and kidney tissues demonstrated that HO-1 protein levels are increased

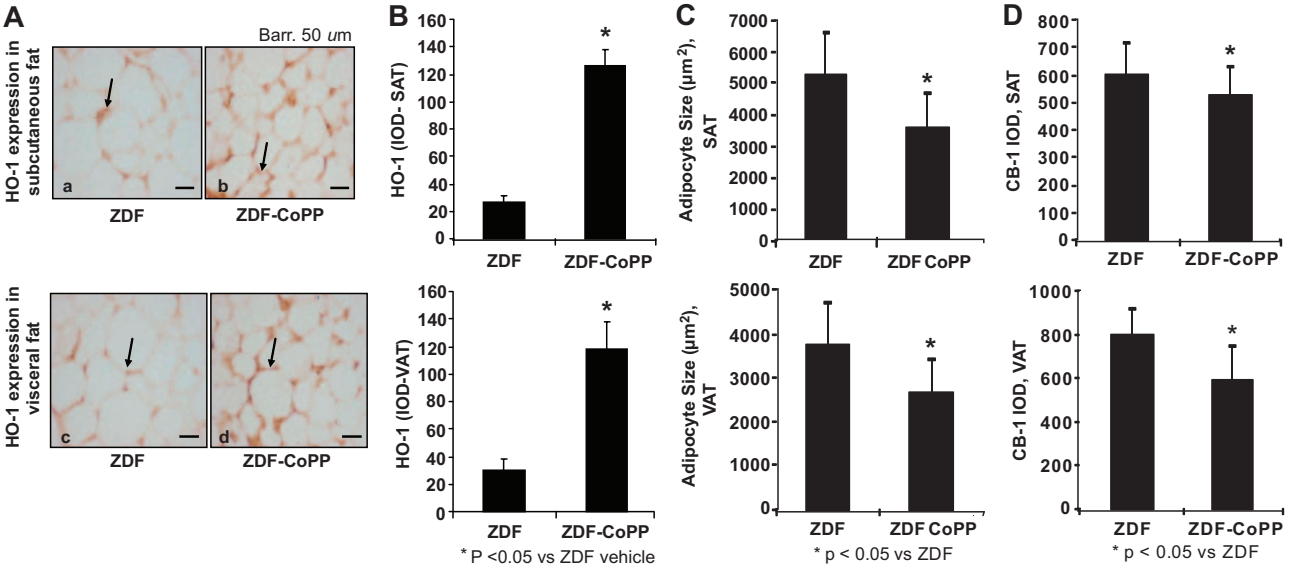

Figure 5. A and B, Immunostaining for HO-1 expression (arrows) in SAT (Aa and Ab) and VAT (Ac and Ad) from ZDF (Aa and Ac) and ZDF–CoPP (Ab and Ad) rats. B, CoPP treatment increases HO-1 expression in SAT and VAT. C, HO-1 induction resulted in significantly smaller adipocytes in the SAT and VAT of ZDF rats and (D) IOD after immunostaining for the CB-1 receptor in subcutaneous and visceral aortic adipose tissues from ZDF and ZDF–CoPP rats. *$P<0.05$ control vs diabetic animals; mean±SE; n=40.

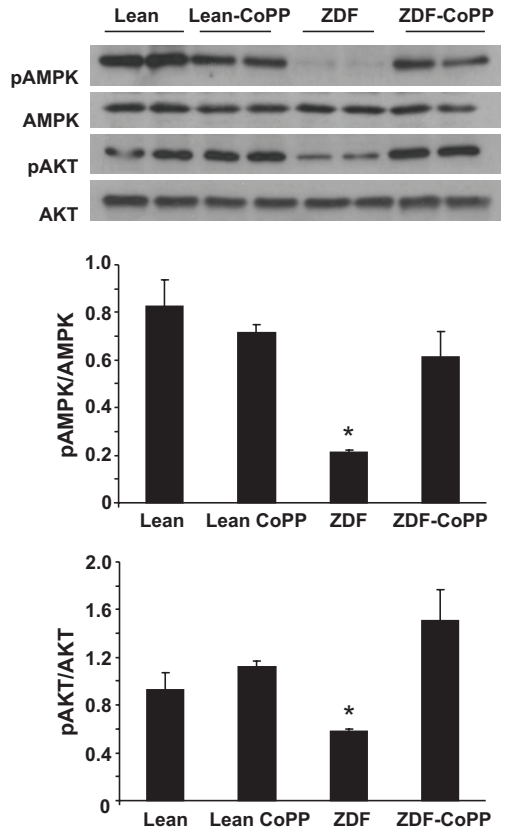

Figure 6. Western blot and densitometry analysis of effect of HO-1 expression on pAKT and total AKT in proteins of aortas from lean, lean–CoPP, ZDF, and ZDF–CoPP rats. Quantitative densitometry evaluation of pAMPK and pAKT in the aorta was determined. *$P<0.05$. Diabetic–obese vs control or diabetic–obese-CoPP. Each bar represents mean±SE of 4 experiments.

but that HO-1 activity is reduced in the ZDF rat compared with lean controls, and that treatment with CoPP drastically increases HO-1 activity in ZDF animals. These findings are in agreement with previous studies of HO-1 expression and activity in the ZDF model.[26] Similarly, adiponectin secretion was reduced significantly in ZDF rats compared with lean, which was again dramatically reversed with CoPP treatment and HO-1 induction. As postulated previously, the effect of HO-1 induction on adiponectin secretion may be attributable to the role of HO-1 as a stress response/chaperone protein, as well as to its antioxidant effects.[6,8,27]

Serum insulin levels, which were elevated in the ZDF rat, were restored to normal with induction of the HO-1 system. In addition, blood glucose levels dropped markedly in response to exogenous insulin administration after HO-1 induction. Both of these results indicate improved insulin sensitivity in ZDF rats treated with CoPP. In the 2007 study by Kim et al,[4] obese diabetic mice that had been transgenically modified to overexpress adiponectin showed significant improvement in insulin sensitivity. Thus, the increased insulin sensitivity we observed may be adiponectin mediated, possibly because of increased expression of the GLUT-4 receptor, as well as to decreased inflammation and reactive oxygen species generation attributable to the antioxidant effects of HO.

The improvement in insulin sensitivity may also have been linked to decreased inflammation in the adipose tissue of rats treated with CoPP. HO-1/adiponectin induction led to histological changes in adipose tissue appearance largely characterized by dramatically lower average adipocyte size. It has been proposed that smaller adipocyte size represents healthier adipose tissue with decreased macrophage infiltration and inflammation.[4,28] Other studies suggested that adiponectin acts as a starvation signal when adipocyte size is small to upregulate adipose tissue accumulation of triglycerides.[4,29] It is not completely clear from our data whether adipocyte size is smaller because of higher levels of circulating adiponectin or whether adiponectin levels increase in response to smaller adipocytes, although this is certainly a relationship that bears further study.

In addition to smaller adipocyte size, there was a marked decrease in weight gain observed in ZDF rats treated with CoPP. Although both SAT and VAT masses were reduced with HO-1 induction, the reduction in VAT mass was greater than the reduction in SAT mass. This was supported by MRI evaluation of SAT and VAT volumes, which demonstrated a decrease in the VAT/SAT ratio consistent with a greater loss of VAT than of SAT. A spectrum of compounds has been shown to upregulate HO-1 expression such as statins, AG1067, and apolipoprotein A-I mimetic peptides L-4F and D-4F.[30–32] D-4F and L-4F, synthesized from amino acids,[29] are potent inducers of HO-1 that decrease superoxide and increase extracellular superoxide dismutase.[16,32] Recently, L-4F treatment has been shown to reduce adiposity, increase adiponectin levels, and improve insulin sensitivity in obese mice.[13] Whatever the mechanism by which HO-1 induction reduces adiposity, the resultant decrease in the relative amount of VAT is significant because VAT appears to play a greater role in obesity-induced insulin resistance than does SAT. There are several possible mechanisms that may have contributed to this phenomenon. One possible explanation is that in the presence of increased adiponectin levels, the distribution of adipose tissue deposition was shifted preferentially from visceral depots to subcutaneous depots. Again, the 2007 study by Kim et al demonstrated a virtually unlimited expansion of SAT in the presence of elevated circulating adiponectin levels without a similar expansion of VAT.[4]

Another possible mechanism involves CB-1 receptor expression. Obesity has been shown to increase activity in the peripheral endocannabinoid system, with increased CB-1 expression and signaling resulting in visceral fat accumulation, decreased adiponectin secretion, and hyperglycemias.[33,34] Our data reflect a decrease in CB-1 receptor expression after HO-1 induction, which may contribute to lower VAT accumulation in ZDF animals.

A large body of evidence demonstrates that pAMPK signaling participates in the regulation of energy balance at both the cellular and systemic levels, downregulating ATP-consuming, anabolic processes and upregulating ATP-producing, catabolic processes.[19,21] AMPK activation is known to reduce inflammation and improve insulin sensitivity and glucose tolerance.[35,36] Therefore, it is significant that pAMPK seems to be reduced in obesity-induced insulin-resistant states and that HO-1–adiponectin induction with CoPP appears to improve AMPK phosphorylation. Similarly, the

present data do not permit us to identify conclusively the molecular mechanism underlying increased eNOS expression resulting from HO-1 upregulation (data not shown). However, ≈2 points must be considered. First, CoPP treatment significantly improves insulin sensitivity. Second, in contrast, circulating adiponectin levels were increased. This finding confirms previous observations[6,8] and seems of particular relevance because adiponectin has been reported to possess a vascular protective role,[37] preserve endothelial cell function in diabetic subjects, increase eNOS activity, and reduce the expression of eNOS inhibitors such as tumor necrosis factor-α.[27] The association of increased serum adiponectin levels and increased stem cell homing[27] and preservation of vascular function closely fits with previous findings by Ouchi et al who, reported a critical role for adiponectin in endothelial cell survival and function[38] via activation of eNOS, pAKT, and pAMPK. These enzymes enhance phosphorylated eNOS levels,[24,39,40] suggesting that restoration of vascular function in obesity and diabetes is a result of the reprogramming of specific metabolic pathways and their signaling components, such as HO-1, pAKT, pAMPK, and phosphorylated eNOS, in a manner that enhances vascular function in Zucker diabetic obese rats.

Perspectives

This study extends our previous findings of HO-1 induction effects on adiponectin secretion and obesity-associated inflammation to include its consequences on insulin resistance and adipose tissue volume, distribution, and structure. The HO–adiponectin system appears to exert encouraging beneficial effects on these consequences of obesity, especially because this study demonstrates upregulation of pAMPK and downregulation of the peripheral endocannabinoid system, the focus of much attention in the science of weight loss. A deeper understanding of the mechanisms involved will provide new approaches for the treatment of obesity, diabetes, and atherosclerosis and improve the effectiveness of cell-based treatment of vascular diseases.

Acknowledgments

The authors are indebted to Daniele DeMarchi and Dr Alessandro Pingipore for their valuable help in the acquisition of MRI data.

Sources of Funding

This work was supported by National Institutes of Health grants DK068134, HL55601, and HL34300, and by a grant from the Beatrice Renfield Foundation (A.K.). This work was also supported by the Consiglio Nazionale delle Ricerche (CNR) Medical Department and Cardiopulmonary Project and the Scuola Sant'Anna.

Disclosures

None.

References

1. Lafontan M, Girard J. Impact of visceral adipose tissue on liver metabolism Part I: Heterogeneity of adipose tissue and functional properties of visceral adipose tissue. *Diabetes Metab*. 2008;34:317–327.
2. Lin Y, Berg AH, Iyengar P, Lam TK, Giacca A, Combs TP, Rajala MW, Du X, Rollman B, Li W, Hawkins M, Barzilai N, Rhodes CJ, Fantus IG, Brownlee M, Scherer PE. The hyperglycemia-induced inflammatory response in adipocytes: the role of reactive oxygen species. *J Biol Chem*. 2005;280:4617–4626.
3. Hotamisligil GS, Shargill NS, Spiegelman BM. Adipose expression of tumor necrosis factor-alpha: direct role in obesity-linked insulin resistance. *Science*. 1993;259:87–91.
4. Kim JY, van de WE, Laplante M, Azzara A, Trujillo ME, Hofmann SM, Schraw T, Durand JL, Li H, Li G, Jelicks LA, Mehler MF, Hui DY, Deshaies Y, Shulman GI, Schwartz GJ, Scherer PE. Obesity-associated improvements in metabolic profile through expansion of adipose tissue. *J Clin Invest*. 2007;117:2621–2637.
5. Osei-Hyiaman D, DePetrillo M, Pacher P, Liu J, Radaeva S, Batkai S, Harvey-White J, Mackie K, Offertaler L, Wang L, Kunos G. Endocannabinoid activation at hepatic CB1 receptors stimulates fatty acid synthesis and contributes to diet-induced obesity. *J Clin Invest*. 2005;115:1298–1305.
6. Kim DH, Burgess AP, Li M, Tsenovoy PL, Addabbo F, McClung JA, Puri N, Abraham NG. Heme oxygenase-mediated increases in adiponectin decrease fat content and inflammatory cytokines, tumor necrosis factor-alpha and interleukin-6 in Zucker rats and reduce adipogenesis in human mesenchymal stem cells. *J Pharmacol Exp Ther*. 2008;325:833–840.
7. Ollinger R, Yamashita K, Bilban M, Erat A, Kogler P, Thomas M, Csizmadia E, Usheva A, Margreiter R, Bach FH. Bilirubin and biliverdin treatment of atherosclerotic diseases. *Cell Cycle*. 2007;6:39–43.
8. Li M, Kim DH, Tsenovoy PL, Peterson SJ, Rezzani R, Rodella LF, Aronow WS, Ikehara S, Abraham NG. Treatment of obese diabetic mice with a heme oxygenase inducer reduces visceral and subcutaneous adiposity, increases adiponectin levels, and improves insulin sensitivity and glucose tolerance. *Diabetes*. 2008;57:1526–1535.
9. Tucci M, McDonald RJ, Aaronson R, Graven KK, Farber WH. Specificity and uniqueness of endothelial cell stress responses. *Am J Physiol*. 1996;271:L341–L348.
10. Positano V, Gastaldelli A, Sironi AM, Santarelli MF, Lombardi M, Landini L. An accurate and robust method for unsupervised assessment of abdominal fat by MRI. *J Magn Reson*. 2004;20:684–689.
11. Demerath EW, Ritter KJ, Couch WA, Rogers NL, Moreno GM, Choh A, Lee M, Remsberg K, Czerwinski SA, Chumlea WC, Siervogel RM, Towne B. Validity of a new automated software program for visceral adipose tissue estimation. *Int J Obes (Lond)*. 2007;31:285–291.
12. Bonekamp S, Ghosh P, Crawford S, Solga SF, Horska A, Brancati FL, Diehl AM, Smith S, Clark JM. Quantitative comparison and evaluation of software packages for assessment of abdominal adipose tissue distribution by magnetic resonance imaging. *Int J Obes (Lond)*. 2008;32:100–111.
13. Peterson SJ, Drummond G, Hyun KD, Li M, Kruger AL, Ikehara S, Abraham NG. L-4F treatment reduces adiposity, increases adiponectin levels and improves insulin sensitivity in obese mice. *J Lipid Res*. 2008;49:1658–1669.
14. Zhang F, Kaide J, Wei Y, Jiang H, Yu C, Balazy M, Abraham NG, Wang W, Nasjletti A. Carbon monoxide produced by isolated arterioles attenuates pressure-induced vasoconstriction. *Am J Physiol*. 2001;281:H350–H358.
15. Abraham NG, Jiang H, Balazy M, Goodman AI. Methods for measurements of heme oxygenase (HO) isoforms-mediated synthesis of carbon monoxide and HO-1 and HO-2 proteins. *Methods Mol Med*. 2003;86:399–411.
16. Peterson SJ, Husney D, Kruger AL, Olszanecki R, Ricci F, Rodella LF, Stacchiotti A, Rezzani R, McClung JA, Aronow WS, Ikehara S, Abraham NG. Long-term treatment with the apolipoprotein A1 mimetic Peptide increases antioxidants and vascular repair in type I diabetic rats. *J Pharmacol Exp Ther*. 2007;322:514–520.
17. L'Abbate A, Neglia D, Vecoli C, Novelli M, Ottaviano V, Baldi S, Barsacchi R, Paolicchi A, Masiello P, Drummond G, McClung J, Abraham N. Beneficial effect of heme oxygenase-1 expression in myocardial ischemia-reperfusion increases adiponectin in mildly diabetic rats. *Am J Physiol*. 2007;293:H3532–H3541.
18. Di Noia MA, Van DS, Palmieri F, Yang LM, Quan S, Goodman AI, Abraham NG. Heme oxygenase-1 enhances renal mitochondrial transport carriers and cytochrome C oxidase activity in experimental diabetes. *J Biol Chem*. 2006;281:15687–15693.
19. Hardie DG. Minireview: the AMP-activated protein kinase cascade: the key sensor of cellular energy status. *Endocrinology*. 2003;144:5179–5183.
20. Skurk C, Maatz H, Kim HS, Yang J, Abid MR, Aird WC, Walsh K. The Akt-regulated forkhead transcription factor FOXO3a controls endothelial cell viability through modulation of the caspase-8 inhibitor FLIP. *J Biol Chem*. 2004;279:1513–1525.

21. Hardie DG. AMP-Activated protein kinase as a drug target. *Annu Rev Pharmacol Toxicol*. 2007;47:185–210.
22. Kurth-Kraczek EJ, Hirshman MF, Goodyear LJ, Winder WW. 5′AMP-activated protein kinase activation causes GLUT4 translocation in skeletal muscle. *Diabetes*. 1999;48:1667–1671.
23. Stoppani J, Hildebrandt AL, Sakamoto K, Cameron-Smith D, Goodyear LJ, Neufer PD. AMP-activated protein kinase activates transcription of the UCP3 and HKII genes in rat skeletal muscle. *Am J Physiol*. 2002; 283:E1239–E1248.
24. Dimmeler S, Fleming I, Fisslthaler B, Hermann C, Busse R, Zeiher AM. Activation of nitric oxide synthase in endothelial cells by Akt-dependent phosphorylation. *Nature*. 1999;399:601–605.
25. Li M, Peterson S, Husney D, Inaba M, Guo K, Terada E, Morita T, Patil K, Kappas A, Ikehara S, Abraham NG. Interdiction of the diabetic state in NOD mice by sustained induction of heme oxygenase: possible role of carbon monoxide and bilirubin. *Antioxid Redox Signal*. 2007;9:855–863.
26. Kruger AL, Peterson SJ, Schwartzman ML, Fusco H, McClung JA, Weiss M, Shenouda S, Goodman AI, Goligorsky MS, Kappas A, Abraham NG. Up-regulation of heme oxygenase provides vascular protection in an animal model of diabetes through its antioxidant and antiapoptotic effects. *J Pharmacol Exp Ther*. 2006;319:1144–1152.
27. Abraham NG, Kappas A. Pharmacological and clinical aspects of heme oxygenase. *Pharmacol Rev*. 2008;60:79–127.
28. Cinti S, Mitchell G, Barbatelli G, Murano I, Ceresi E, Faloia E, Wang S, Fortier M, Greenberg AS, Obin MS. Adipocyte death defines macrophage localization and function in adipose tissue of obese mice and humans. *J Lipid Res*. 2005;46:2347–2355.
29. Florant GL, Porst H, Peiffer A, Hudachek SF, Pittman C, Summers SA, Rajala MW, Scherer PE. Fat-cell mass, serum leptin and adiponectin changes during weight gain and loss in yellow-bellied marmots (*Marmota flaviventris*). *J Comp Physiol B*. 2004;174:633–639.
30. Hsu M, Muchova L, Morioka I, Wong RJ, Schroder H, Stevenson DK. Tissue-specific effects of statins on the expression of heme oxygenase-1 in vivo. *Biochem Biophys Res Commun*. 2006;343:738–744.
31. Stocker R, Perrella MA. Heme oxygenase-1: a novel drug target for atherosclerotic diseases? *Circulation*. 2006;114:2178–2189.
32. Kruger AL, Peterson S, Turkseven S, Kaminski PM, Zhang FF, Quan S, Wolin MS, Abraham NG. D-4F induces heme oxygenase-1 and extracellular superoxide dismutase, decreases endothelial cell sloughing, and improves vascular reactivity in rat model of diabetes. *Circulation*. 2005; 111:3126–3134.
33. Akbas F, Gasteyger C, Sjodin A, Astrup A, Larsen TM. A critical review of the cannabinoid receptor as a drug target for obesity management. *Obes Rev*. 2008. Aug 20. [Epub ahead of print].
34. Engeli S, Bohnke J, Feldpausch M, Gorzelniak K, Janke J, Batkai S, Pacher P, Harvey-White J, Luft FC, Sharma AM, Jordan J. Activation of the peripheral endocannabinoid system in human obesity. *Diabetes*. 2005; 54:2838–2843.
35. Bandyopadhyay GK, Yu JG, Ofrecio J, Olefsky JM. Increased malonyl-CoA levels in muscle from obese and type 2 diabetic subjects lead to decreased fatty acid oxidation and increased lipogenesis; thiazolidinedione treatment reverses these defects. *Diabetes*. 2006;55:2277–2285.
36. Yang X, Ongusaha PP, Miles PD, Havstad JC, Zhang F, So WV, Kudlow JE, Michell RH, Olefsky JM, Field SJ, Evans RM. Phosphoinositide signaling links O-GlcNAc transferase to insulin resistance. *Nature*. 2008; 451:964–969.
37. Hopkins TA, Ouchi N, Shibata R, Walsh K. Adiponectin actions in the cardiovascular system. *Cardiovasc Res*. 2007;74:11–18.
38. Ouchi N, Kobayashi H, Kihara S, Kumada M, Sato K, Inoue T, Funahashi T, Walsh K. Adiponectin stimulates angiogenesis by promoting cross-talk between AMP-activated protein kinase and Akt signaling in endothelial cells. *J Biol Chem*. 2004;279:1304–1309.
39. Chen ZP, Mitchelhill KI, Michell BJ, Stapleton D, Rodriguez-Crespo I, Witters LA, Power DA, Ortiz De Montellano PR, Kemp BE. AMP-activated protein kinase phosphorylation of endothelial NO synthase. *FEBS Lett*. 1999;443:285–289.
40. Jantzen F, Konemann S, Wolff B, Barth S, Staudt A, Kroemer HK, Dahm JB, Felix SB, Landsberger M. Isoprenoid depletion by statins antagonizes cytokine-induced downregulation of endothelial nitric oxide expression and increases NO synthase activity in human umbilical vein endothelial cells. *J Physiol Pharmacol*. 2007;58:503–514.